LABORATORI NAZIONALI DI FRASCATI
SIS – Pubblicazioni

LNF–95/032 (IR)
22 Giugno 1995

# Theoretical Parameters of a Pseudo–Spherical Stepped x–ray Diffractor

M.I. Mazuritsky, A.V. Soldatov, I.E. Stekhin
Department of Solid State Physics, Rostov University, Rostov–Don, 344104 Russia

A. Marcelli
INFN, Laboratori Nazionali di Frascati, P.O.Box 13, 00044 Frascati, Italy

**Abstract**

A novel type of x–ray diffractor based on a pseudo–spherical stepped geometry is proposed. Theoretical parameters of three possible devices based on this geometry, a high–resolution 'post' monochromator for spin–dependent x–ray absorption, a x–ray microanalyser and a x–ray photoelectron spectrometer for chemical analysis (ESCA), are discussed. The efficiency of this flexible optical scheme for each one of these x–ray devices is calculated and found to improve substantially the existing devices based on the spherical geometry.

**PACS.: 07.85.+n; 29.30.Kv; 82.80.Ej**

## I. INTRODUCTION

In many x–ray spectral devices, x–ray characteristic radiation is generated by a small area out of the entire sample surface. In such a case the source can be considered point–like, this is the case, e.g., of a x–ray scanning microanalyser or a x–ray spectral apparatus employing focused primary x–ray radiation. For instance, in the x–ray CAMEBAX microanalyser with 160 mm focal circle radius the size of the electron probe is approximately 2 mm of diameter. The conventional focusing technique is made either by a cylindrically curved crystal (Johann method [1]) or by doubly curved on spherical or toroidal surface crystal monochromators. These diffractors focus the monochromatic radiation onto the entrance slit of the detector. According to Bragg's equation, the spectral resolution $\Delta\lambda/\lambda$ of the systems, depends both on $\theta$ and $\Delta\theta$:

$$\Delta\lambda/\lambda=\Delta\theta/\tan\theta \qquad (1)$$

The intensity of the monochromatic radiation is proportional to the area of the diffractor surface that reflects the x–rays under the given Bragg's angle $\theta$ within the range $\pm\Delta\theta$. However, by increasing the area a widening of the aperture ratio of the diffractor occurs which is associated to a simultaneous decrease of the spectral resolution.

In the last decade analytic investigations on shape and size of the reflecting area of a crystal–monochromator surface employing different focusing methods, have been carried out [2–5]. Indeed, x–ray diffractors with a double curved crystal, provide significantly greater aperture ratios compared to that obtained in Johann geometry. For a device with an incidence angle $\theta>20°$ and a crystal height $L<0.1R$, the reflecting surface projection on the $XZ$ plane, is rectangular and the projection on the focal circle plane ($XY$ plane) is an arc of radius $R=2r$, where $r$ is the focal circle radius. The shape of the reflecting surface allows to estimate the parameters for a pseudo–spherical diffractor with a stepped surface [4] and, in the case of constant step height, the aperture of this diffractor is shown to exceed that of a spherical curved crystal diffractor by several times.

In the present work a stepped diffractor based on different step condition with a constant angle width ($\varphi$–const) has been considered. We will demonstrate that the efficiency of this diffractor is superior to that of a similar diffractor designed with the constant step height ($h$–const condition). The dependence of the diffractor aperture on the Bragg's angle and the magnitude of resolution will also be presented. Moreover, the diffractor parameters of three different x–ray spectral diffractor devices will be discussed.

## II. DIFFRACTOR LAYOUT AND PARAMETERS

Figure 1 shows the scheme of the stepped surface diffractor projected into the focal plane. In the $XZ$ plane each step is a strip of length $L$ (crystal height) along the $z$–axis. The step lies on a spherical surface of radius $R_i$ where $R_i = OA_i$, O' is the center of the focal circle and $h_i = B_iD_i$ is the height of the $i$–th step. In the plane of Fig. 1 the steps are shown as arcs of size $2\varphi_i = 2(A_iB_i)$, where $i$ = 0, 1,..., N.

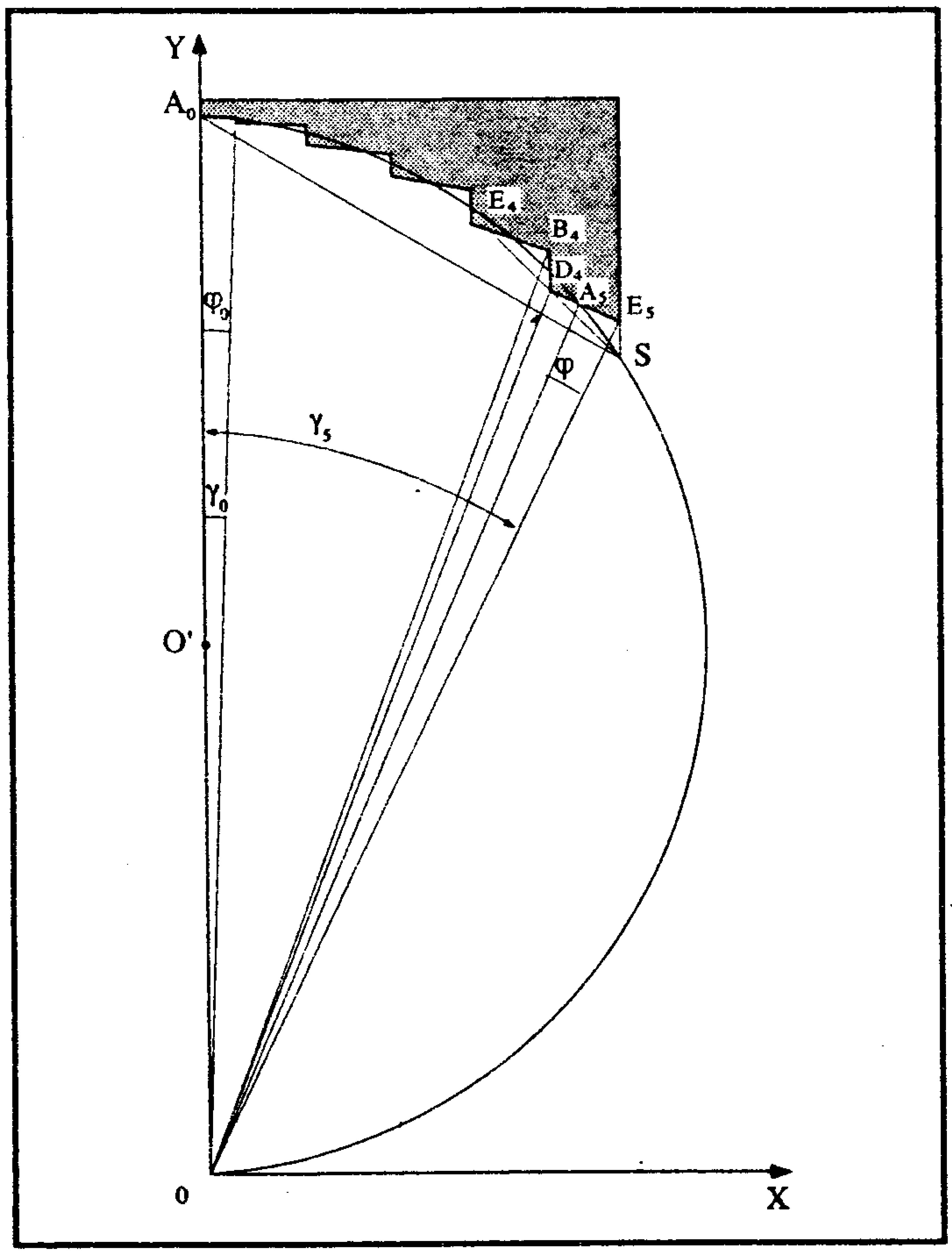


**FIG. 1** – Scheme of the stepped surface diffractor under the $\varphi$=const condition ($\varphi$ is the half width–angle of the $i$–th step) in the focusing circle plane. $OA_0 = R_0 = 2r$ where $r$ is the focusing circle radius; $A_i$ is the point of intersection between $i$–th step surface and the focal circle; $OA_i$ is the curvature radius of the $i$–th step; $B_iD_i = h_i$ is the height of the $i$–th step; S is the focusing point; O' is the centre of the focal circle; and $E_iB_i$ is the portion of the $i$–th step shadowed by the $(i+1)$–th step.

In the following we present the calculation scheme for this diffractor. The value of $\Delta\theta$ was calculated for given magnitudes of $\lambda$, $\Delta\lambda$ and $\theta$. The initial value $\varphi_0 = \gamma_0$ was determined by using the following equation (Ref. 2)

$$2\Delta\theta = X^2 \cot\theta + X^3 \cot^2\theta - XZ^2 \cot^2\theta \qquad (2)$$

Equation 2 determines the coordinates of the boundaries of the reflection area on the spherical crystal surface. Radius $R_0 = 2r$ establishes the curvature of the central step. When the focal circle radius $r$ is fixed, the parameters of the other steps are evaluated by using the following formulae:

$$R_i = R_{i-1} \sin(\gamma_{i-1}) / \sin(\Delta_i) \qquad (3a)$$

$$\tan(\alpha_i) = \sqrt{R_0^2 - R_i^2} / R_i \qquad (3b)$$

$$\gamma_i = \alpha_i + \varphi_i \qquad (3c)$$

$$\varphi_i = \alpha_i - \Delta_i \tag{3d}$$

where $\alpha_i = A_0OA_i$ , $\Delta_i = A_0OD_i$, $\gamma_i = A_0OB_i$ and $\varphi_i = A_iOB_i$ (i>=1). The magnitude of $\Delta_i$ is function of the model. For a diffractor designed under the constraint with *h*=const, it is

$$\tan \Delta_i = R_{i-1}\sin(\gamma_{i-1}) / (R_{i-1}\cos(\gamma_{i-1}) - h) \tag{4}$$

while for our proposed diffractor $\Delta_i$ is evaluated by using an iterative method according to each different $\varphi$=const condition. The source is located on the focal circle, so that the half–width angle of the diffractor on the focal plane, excluding the areas where shadow effect occurs, is calculated as:

$$\Omega = 2(\Omega_0 + \sum_{i=0}^{N} \Omega_i) \tag{5}$$

$\Omega_0 = A_0SE_0$ and $\Omega_i = D_{i-1}SE_i$. Taking into account the increase of the angle width of the reflecting surface, the diffractor aperture ratio is given by the central step aperture times the factor $\Omega/\Omega_0$.

## III. RESULTS AND DISCUSSIONS.

Table I reports the results obtained for both the *h*– and $\varphi$–const conditions. In order to compare the two models we performed calculations with the same set of parameters discussed in Ref. 4, i.e., focal circle radius *r*=50 mm, Bragg's angle $\theta$=22.76°, *h*=0.15 mm and central step width 3.87 mm. For the *h*–const condition the step number increases as its size decreases. As a consequence, the diffractor aperture of the $\varphi$–const diffraction is bigger because of the large size of the device, i.e., for *i*=7, $B_x$ increases from 15.05 mm to 38.60 mm, despite the step being the same in both cases. Comparative studies for different kinds of diffractor devices support the advantage of a device based on the $\varphi$–const approximation.

One of the most important and interesting property of a stepped diffractor at $\varphi$–const condition is that increasing the aperture ratio does not determine reduction of the resolution. As a matter of fact in some cases (Fig. 2) both a high aperture ratio and a high resolution arise. This advantageous condition is fulfilled for different Bragg's angles and focal circle radii. Fig. 3 reports the dependence of the diffractor aperture on the Bragg's angle for resolution parameters in the range $5\ 10^{-5} < \Delta\lambda/\lambda < 10^{-4}$. This interval corresponds to the range of modern high resolution spectrometers [7,8] and coincide with the typical silicon rocking curve width (5") [9] in the angular range 25°<$\theta$<45°. This curve shows a sharp maximum at $\theta$=44°, and a significant increase in aperture occurs at $\theta$=42°, 43° and 45°. However, the average value of the aperture in this range is always greater than 0.058 sr with variations in the range of 15%.

**TABLE I** – Theoretical parameters for two stepped diffractors: h–const model [4] and φ–const model (see text).

| i | h=0.15 mm (h-const) | | | φ=1.6° (φ-const) | | |
|---|---|---|---|---|---|---|
| | $R_i$(mm) | φ(deg) | $B_x$(mm) | $R_i$(mm) | $h_i$(mm) | $B_x$(mm) |
| 0 | 100.0 | 2.22 | 3.87 | 100.0 | 0.00 | 2.81 |
| 1 | 99.9 | 0.92 | 7.06 | 99.8 | 0.16 | 8.46 |
| 2 | 99.7 | 0.37 | 8.36 | 99.4 | 0.47 | 13.81 |
| 3 | 99.6 | 0.61 | 10.49 | 98.6 | 0.78 | 19.09 |
| 4 | 99.4 | 0.22 | 11.23 | 97.5 | 1.12 | 24.23 |
| 5 | 99.3 | 0.52 | 12.99 | 96.0 | 1.50 | 29.25 |
| 6 | 99.1 | 0.14 | 13.48 | 94.2 | 1.96 | 34.05 |
| 7 | 99.0 | 0.46 | 15.05 | 91.8 | 2.52 | 38.60 |

i – step number (starting from the middle of the diffractor – Fig. 1);
$R_i$ – radius of *i*–th step;
φ – half width angle of the *i*–th step;
$h_i$ – height of the *i*–th step ($h_i=B_iD_i$ is the distance from the end of the *i*–th step to the beginning of next step ($i+1$) along *OY* – Fig. 1);
$B_x$ – *x* coordinate of the end of the *i*–th step.

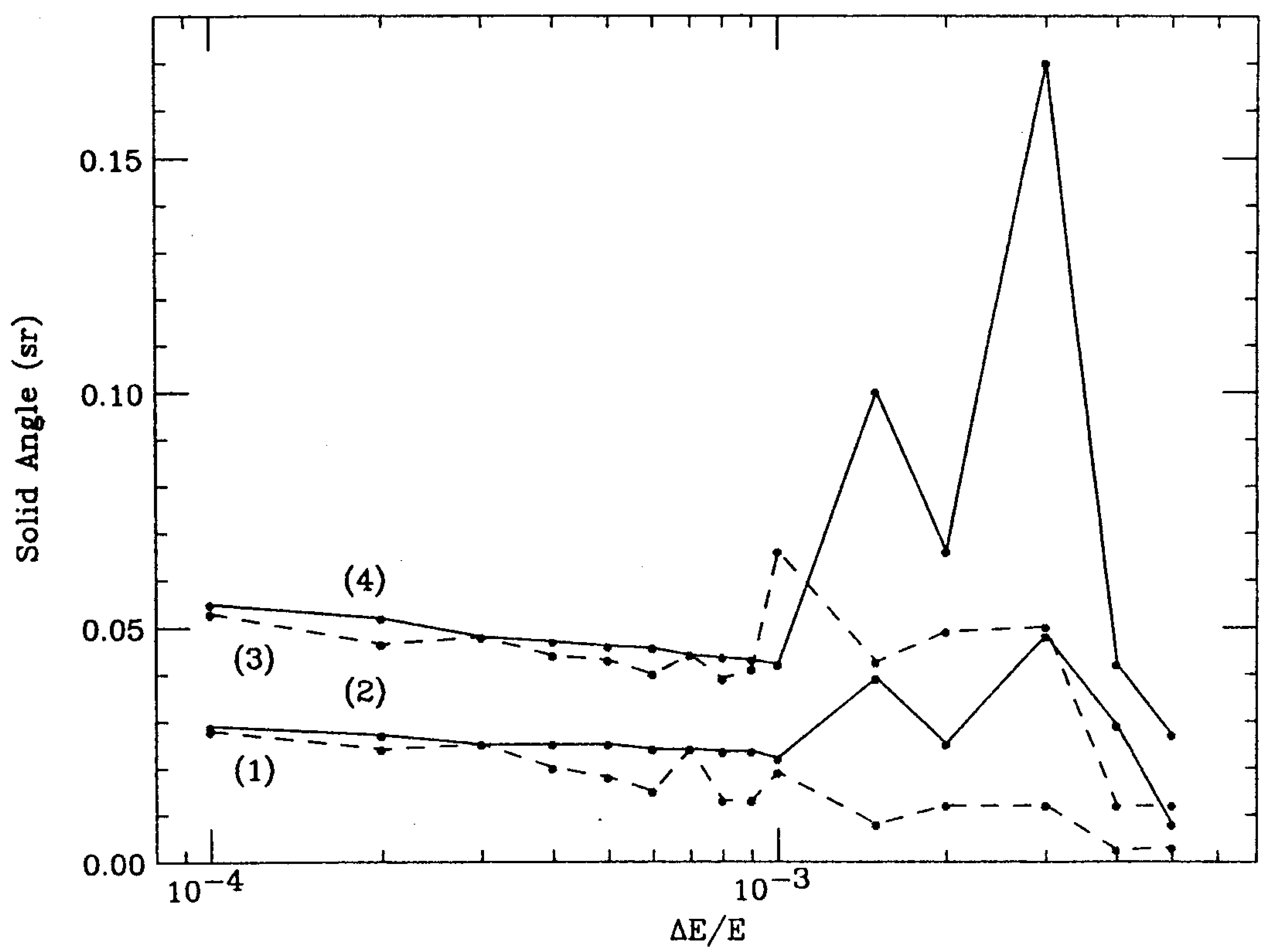


**FIG. 2** – Angular aperture of a stepped diffractor built under the φ=const condition as a function of resolution. Curves 1 and 3 correspond to θ=45°; curves 2 and 4 to θ=30°. Curves 1 and 2 are calculated for a focusing circle of $r$=160 mm and a diffractor height of $L$=16 mm, while curves 3 and 4 are calculated for a focusing circle of $r$=100 mm and a diffractor height of $L$=100 mm.

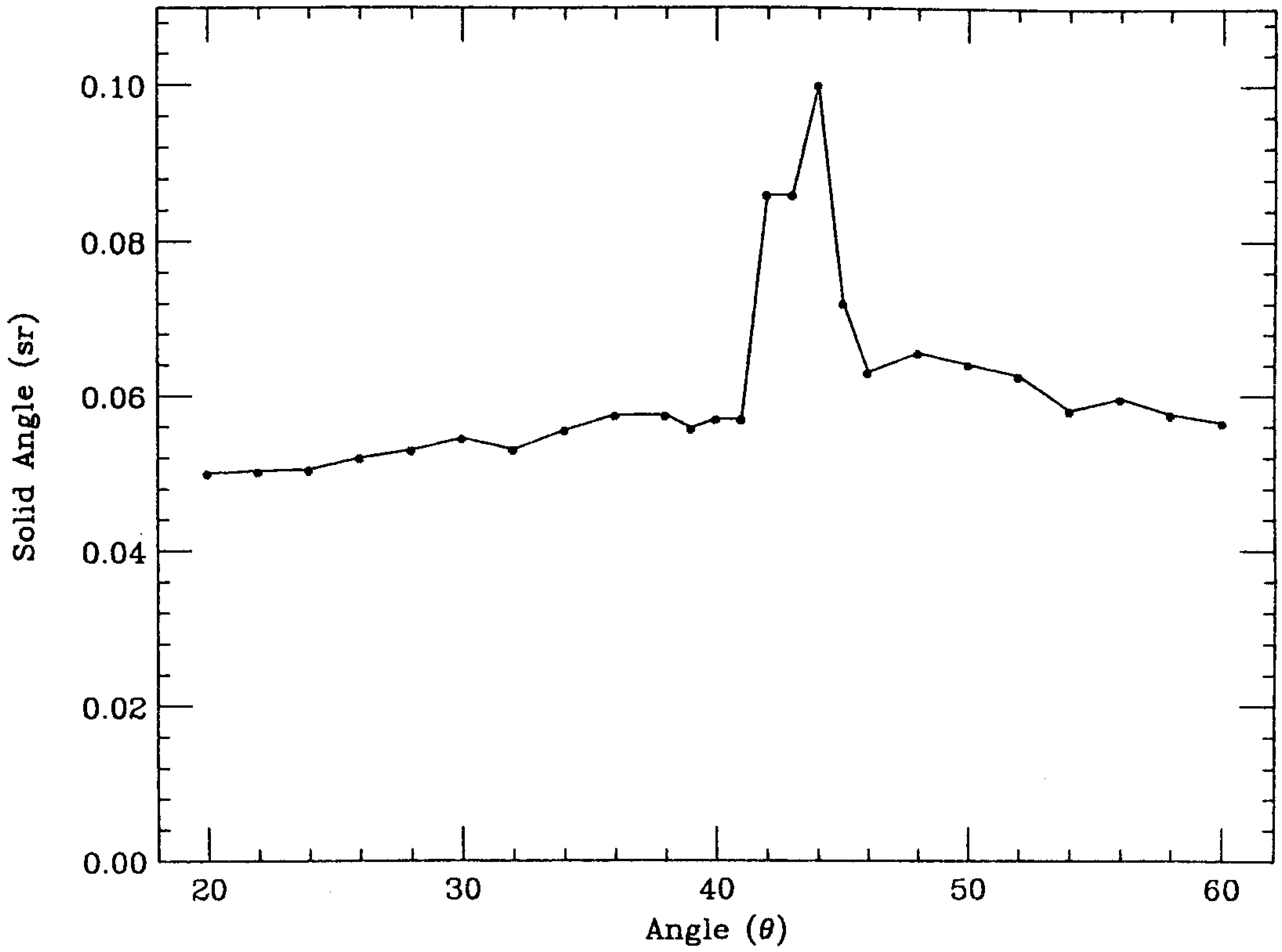


**FIG. 3** – Acceptance of a stepped diffractor device as a function of the Bragg's angle in the resolution range $5\ 10^{-5}<\Delta\lambda/\lambda<10^{-4}$.

Table II reports the parameters of a diffractor for x–ray absorption near edge spectra (XANES) at the Ce $L_2$–edge ($\lambda$=2.012 Å) having resolution of ~$9\ 10^{-5}$ and a focal circle radius $r$=400 mm. To provide the focusing conditions, thin crystals (0.2-0.5 mm) of Si (220), primarily cut into strips according to the step size and curved and glued on a spherical surface may be used as diffraction elements. The Bragg's angle corresponds to the value $2d$=3.84 Å [9] and the aperture is equal to 0.065 sr for a vertical size of the device of $L$=100 mm. Such a spectrometer exhibits an aperture ratio more than 50 times larger than a spherically curved crystal. Calculation also shows that an angular scanning of the spectrum in ±1° range from the given value of θ=31.6° changes the resolution and the aperture ratio by only 2%. However, this small angular range is enough to measure a typical XANES spectrum, since it corresponds to an interval of ~300 eV. To obtain XANES spectra of other chemical elements i.e., at different energy, it is necessary to substitute the above diffractor with another set of crystals, or to change the Bragg's angle.

Other kind of x–ray devices widely used are x–ray microanalysers. These last need a high aperture ratio but are not so demanding in resolution ($\Delta\lambda/\lambda>10^{-3}$). For these instruments the diffractor surface could use plates of muscovite (mica), which provides high plasticity. In Tables III and IV diffractor parameters for a microanalyser CAMEBAX–micro type with 160 mm focal circle radius are reported. To analyze Cu (Z=29) and Ti (Z=22) elements the LiF crystallographic planes (220) and (200) under the Bragg'sangles of 28.96° and of 38.38° respectively should be used. For a diffractor height of $L$=16 mm a great aperture (0.024 sr) associated to a moderate resolution of $\Delta\lambda/\lambda=3\mathrm{x}10^{-4}$ is obtained for the first case, while in the second case an aperture of 0.023 sr and a resolution of $\Delta\lambda/\lambda=5\mathrm{x}10^{-4}$ are calculated. The gain is estimated about 15–30 times depending on the crystal size and the applied focusing technique of the microanalyser channel.

**TABLE II** – Theoretical parameters for a stepped diffractor ($\varphi$–const model) calculated at the Ce $L_2$ absorption edge ($\varphi_0$ =0.47°).

| i | $R_i$ | $B_x$ | $h_i$ |
|---|---|---|---|
| 0 | 800.0 | 6.6 | 0.0 |
| 1 | 799.9 | 19.6 | 0.1 |
| 2 | 799.6 | 32.8 | 0.3 |
| 3 | 799.0 | 46.0 | 0.6 |
| 4 | 798.3 | 58.9 | 0.8 |
| 5 | 797.3 | 71.8 | 1.0 |
| 6 | 796.1 | 84.7 | 1.2 |
| 7 | 794.7 | 97.5 | 1.4 |
| 8 | 793.1 | 110.2 | 1.6 |
| 9 | 791.3 | 122.8 | 1.9 |
| 10 | 789.2 | 135.4 | 2.1 |
| 11 | 786.9 | 147.9 | 2.3 |
| 12 | 784.4 | 160.2 | 2.6 |
| 13 | 781.7 | 172.6 | 2.8 |
| 14 | 778.7 | 184.8 | 3.1 |
| 15 | 775.4 | 196.9 | 3.4 |
| 16 | 771.9 | 208.9 | 3.7 |
| 17 | 768.1 | 220.8 | 4.0 |
| 18 | 764.0 | 232.6 | 4.3 |
| 19 | 759.6 | 244.2 | 4.6 |
| 20 | 754.9 | 255.6 | 5.0 |
| 21 | 749.9 | 267.0 | 5.4 |
| 22 | 744.5 | 278.1 | 5.8 |
| 23 | 738.7 | 289.1 | 6.2 |
| 24 | 732.5 | 299.9 | 6.7 |
| 25 | 725.8 | 310.5 | 7.3 |
| 26 | 718.7 | 320.9 | 7.9 |
| 27 | 710.9 | 331.1 | 8.7 |

(For parameters description see Table I).

**TABLE III** – Theoretical parameters for a stepped diffractor (φ–const model) for a microanalyser at the K edge of Cu ($\varphi_0$ =0.76°).

| i | $R_i$ | $B_x$ | $h_i$ |
|---|---|---|---|
| 0 | 320.0 | 4.2 | 0.00 |
| 1 | 319.9 | 12.4 | 0.11 |
| 2 | 319.6 | 20.7 | 0.32 |
| 3 | 319.0 | 29.0 | 0.55 |
| 4 | 318.3 | 37.2 | 0.77 |
| 5 | 317.3 | 45.3 | 0.99 |
| 6 | 316.1 | 53.3 | 1.21 |
| 7 | 314.7 | 61.2 | 1.44 |
| 8 | 313.0 | 69.0 | 1.70 |
| 9 | 311.1 | 76.8 | 1.96 |
| 10 | 308.9 | 84.4 | 2.24 |
| 11 | 306.5 | 91.9 | 2.53 |
| 12 | 303.8 | 99.2 | 2.86 |
| 13 | 300.7 | 106.5 | 3.24 |
| 14 | 297.3 | 113.5 | 3.64 |
| 15 | 293.5 | 120.4 | 4.11 |

(For parameters description see Table I).

**TABLE IV** – Theoretical parameters for a stepped diffractor (φ–const model) for a microanalyser at the K edge of Ti ($\varphi_0$ =1.45°).

| i | $R_i$ | $B_x$ | $h_i$ |
|---|---|---|---|
| 0 | 320.0 | 8.1 | 0.00 |
| 1 | 319.6 | 24.3 | 0.41 |
| 2 | 318.4 | 40.2 | 1.24 |
| 3 | 316.3 | 55.8 | 2.08 |
| 4 | 313.4 | 71.1 | 2.98 |
| 5 | 309.5 | 85.9 | 3.94 |
| 6 | 304.7 | 100.3 | 5.06 |
| 7 | 298.6 | 114.2 | 6.39 |
| 8 | 291.2 | 127.3 | 8.09 |
| 9 | 281.8 | 139.6 | 10.44 |
| 10 | 269.5 | 150.9 | 14.24 |

(For parameters description see Table I).

**TABLE V** – Theoretical parameters for a stepped diffractor (φ–const model) for an ESCA spectrometer ($\varphi_0$ =1.33°)

| i | $R_i$ | $B_x$ | $h_i$ |
|---|---|---|---|
| 0 | 200.0 | 4.6 | 0.0 |
| 1 | 199.8 | 13.8 | 0.21 |
| 2 | 199.2 | 22.8 | 0.64 |
| 3 | 198.1 | 31.7 | 1.06 |
| 4 | 196.6 | 40.4 | 1.51 |
| 5 | 194.7 | 48.9 | 1.99 |
| 6 | 192.2 | 57.2 | 2.53 |
| 7 | 189.2 | 65.3 | 3.15 |
| 8 | 185.6 | 73.0 | 3.87 |

(For parameters description see Table I).

The above x–ray devices do not represent all the applications of a stepped diffractors. Other experimental apparatus could implement these devices. The characteristic radiation of the x–ray photons (Al *Kα* or Mg *Kα*) of an x–ray photoelectron spectrometer (ESCA), when absorbed by the sample, are known to induce the appearance of free photoelectrons. The intensity and the contrast of x–ray photoelectron spectra are remarkably magnified by intense incident quantum flux. In addition, if the x–ray radiation is focused in a small probe the possibility of local x–ray electron analysis appears. The properties of the stepped surface diffractor like that described above permit to design also new XPS spectrometers allowing high contrast spectra of micro–sample. In Table V the diffractor parameters for an x–ray monochromator at the Mg *Kα* energy ($\lambda$=9.89 Å) are also reported. An acceptance of 0.17 sr is obtained with the following parameters: focal circle radius of $r$=100 mm, diffractor height of $L$=20 mm and resolution $\Delta\lambda/\lambda = 8\ 10^{-4}$. The x–ray beams is diffracted by the muscovite planes (001) at $\theta$=29.90° ($2d$=19.84 Å). This diffractor has only eight steps but the advantage in intensity over a spherical curved crystal is estimated to be about 15 times.

## IV. SUMMARY AND CONCLUSIONS

A new type of pseudo–spherical stepped x–ray diffractor device with step subtending a constant angle width is proposed. The main advantage of this diffractor is that large output is coupled with a good spectral resolution when required.

Detailed geometrical and physical parameters have been presented for three different applications: high resolution 'post' monochromator for spin–dependent x–ray absorption experiments, x–ray microanalyser, and x–ray photoelectron spectrometer for chemical analysis (ESCA).

## ACKNOWLEDGMENTS

It is a pleasure to acknowledge A. Mottana for the stimulating discussion and the critical readings of the manuscript. This research was partially supported by RBRF grant 94–02–03038 and a grant from the Committee for Higher Education of Russia.


## REFERENCES


1. *Advances in X–Ray Spectroscopy*, Eds. C. Bonnelle, C. Mande, (Oxford, U.K., 1982).
2. D.B. Wittry and S. Sun, J. Appl. Phys. **67**, 1633 (1990).
3. D.B. Wittry and S. Sun, J. Appl. Phys. **68**, 387 (1990).
4. D.B. Wittry and S. Sun, J. Appl. Phys. **69**, 3886 (1991).
5. D.B. Wittry and S. Sun, J. Appl. Phys. **71**, 564 (1992).
6. W.Z. Chand and D.B. Wittry, J. Appl. Phys. **74**, 2999 (1993).
7. V. Stojanoff, K. Hämäläinen, D.P. Siddons, J.B. Hastings, L.E. Berman, S. Cramer, G. Smith, Rev. Sci. Instrum. **63**, 1125 (1992).
8. G. Peng, F.M.F. de Groot, K. Hämäläinen, J.A. Moore, X. Wang, M.M. Grush, J.B. Hastings, D.P. Siddons, W.H. Armstrong, O.C. Mullins and S.P. Cramer, J. Am. Chem. Soc. **116**, 2914 (1994).
9. T. Matsushita and H.–O Hashizume, in: *Handbook on Synchrotron Radiation*, ed. E.E. Koch (North–Holland, Amsterdam, 1983) p. 261.